

UHF-RFID ANTENNA FOR SEMI-ACTIVE ASSISTED TAGS

Nicolae CRIȘAN

*Communication Department, Technical University of Cluj-Napoca, Romania
Corresponding author: Nicolae.Crisan@com.utcluj.ro*

Abstract: This paper proposes a new concept of using RFID tag antennas more actively in the identification process. This innovative concept is based on antenna native properties that allow RF harvesting for DC biasing, either from the reader or from other proximity RF sources at the same time. Nevertheless, for now, RFID identification tags without a self-DC power supply have become more popular and are referred to as passive. Eventually, both RF and light harvesting processes could be addressed as a foreseeable solution for identification range extension. Soon this trend will lead to the cheapest (printable) RFID tags at competitive prices closely shifted to those of the already mass-produced barcode tags, mainly in use today. The proposed semi-passive tag antenna is working by replacing the IMPINJ-MONZA chip with the EM4325 chip which can be DC supplied by a PV panel. This tag can work as RF energy harvester and can be DC biased as well, being the most capable for the proposed concept. The antenna is printed on paper using a metal powder ink printer and the tag is interrogated using a UHF-RFID reader. The harvesting for tag DC biasing is extended through a very small solar panel, which acts also as a substrate for the RFID antenna. Thus, the extended concept of the semi-active tag could increase the coverage and the sensing range of the reader significantly. This happens especially in daylight or when other nearby RF sources are available, otherwise, the tag will work as an ordinary one. This approach will allow the antenna to be shrunk even further near the Chu-Harrington limit.

Keywords: Antenna, RFID-tag, radio frequency identification, internet of green things

I. INTRODUCTION

UHF-RFID tagging technique employed scatterer modulation to interrogate and identify tags. Some changes according to amplitude, phase, or signal power involve near-field magnetic or electric coupling through impedance modulation of the tag's antenna according to an ID code. This approach involves the use of RF powers that will be harvested from the reader. Using passive tags only, harvested RF power with the help of the antenna is converted into a DC that is allowing the supply of the tag's chip. Then the impedance modulation of the tag's antenna is triggered using an electronic on/off switch. The mechanism is limited due to the power needed from the source (that is supplied in normal circumstances by the reader alone), and the scattered signals which suffer from attenuation. The reader must closely follow the tag to mitigate those issues. The identification process also requires a protocol [1] that reduces the identification distance due to the scattered signal integrity. The first RFID chipless tag that can store information (in the ID), was revealed by Thomas Thompson in 1956 [2] and it was designed as a system for preventing shoplifting in supermarkets. In this respect, the multi-bit chipless RFID tag technique has been growing up till now using acoustic wave resonators in which case the RFID tag was interrogated by transmitting and receiving only an RF carrier. Receiving a sinusoidal RF carrier signal having a unique spectral signature avoids the need for identification protocols that demand the use of modulations [3]. This approach improves the scattered signal integrity due to its resistance against noise. Even though passive tag detection is not a multi-tag identification capable in the absence of a handshaking mechanism. In comparison to the classic

UHF-RFID detection (which uses a chip for ID identification), the interrogation protocol and modulation technique make multi-tag detection possible. In concordance with recent improvements and trends, even though, new innovative designs and concepts about chipless tags have emerged. Based on SAW (Surface Acoustic Wave) resonators, the development trends are allowing now higher resolution concerning stored bits concept and loss mitigation. A chipless tag behaves like a barcode system which can only identify a single tag at once that is nearby. Nevertheless, in the case of the chipless tag, unlike a barcode system, the identification range and scattered signal integrity are improved significantly. The reader should be able to detect the resonance frequencies from the tag using the scattered signal only. Likewise, the scattered signal could collide with other signals from other tags. This causes interference which is referred to as clutter, and the reader must have a selectively capable filter to identify the signal through the clutter. This selection is based on the strongest scattered signal that is bounced back from the nearest tag. The resemblance to the barcode was highlighted by Imad Jalay in 2005 [4] when more RFID bands were used to reshape the tag frequency signature employing multi-dipoles with different lengths. In this respect, McVay introduced his space-filling curve [5] as a chipless tag and in 2007 Majid Manteghi introduced the concept of an RFID tag with multiple quarter-wavelengths [6] to diversify its frequency signature up to three bits of information stored. However, the main advantage of the chipless tags is related to the fabrication cost due to the availability of new printing techniques based on metallic ink. Though, the main disadvantage of the chipless tags is related to the multi-tag's detection in capability. The UHF-RFID technology is based

on passive tags as well but is multi-tag detection capable. Due to the maturation of RF technology RFIDs will be more present in many applications like deposit management and payments. This paper searches for some methods that allow the antenna to gather more RF energy or at least to extend the energy harvesting from the reader through other sources like RF or even further to extend energy harvesting through antenna integration in/or upon solar panels [7]. In this respect, a solar panel could be integrated into antenna structures and would act as a director or as a reflector. The slots or strips between the solar cells can be exploited to feed the antenna with RF. The DC power generation would help by biasing the tag and extending the detection range. Besides, these studies bring together other approaches along which new materials like AgHT emerge, which introduces the concept of the transparent antenna [8]. Transparent conductors like AgHT-made materials allow more straightforward approaches which could place the antenna in front of the solar panel and use it as an RF radiator or reflector. This technique not only extends the antenna usage but also changes how green energy will be produced in RF small gadgets. Nowadays new materials and technologies that are related especially to nano-material usage become game changers in extending wireless device capabilities. A multirole antenna that besides RF energy conversion exploits other RF sources and IR light harvesting would pave the way to the internet of green things following this approach of semi-active devices rather than ordinary chipless tag rules.

II. ANTENNA DESIGN FOR UHF-RFID TAGS

The Monza R6-P RFID chip is the most important device that stands for DC biasing, demodulation, and signal scattering control. This chip has been chosen due to its capability to automatically adjust its parameters during the detection process. The chip tag has a sensitivity up to -22.1 dBm related to a dipole antenna, this sensing trait coming in combination with an excellent interference rejection, which leads to higher readability. The R6 chip is complying with the second generation of EPC radio frequency identity protocols, referred as to EPC-Class1 Gen2 UHF-RFID. Another trait addresses the auto-tune function. The auto-tuner matches the conjugate input impedance of the chip to the impedance of the antenna to optimize the RF power transfer during operation. This is a special demand for a shrunk antenna that reduces its electric length to a minimum to comprise the labeled size of the tag sticker. Smaller RFID antennas increase in this way the applicability of the tag to a variety of products with different sizes and shapes. The sticker size, which is used to support the antenna, confines inside a rectangle of 6/4 centimeters. In normal circumstances, the electrical length of the dipole antenna at 900 MHz must be up to 16.6 centimeters, which means a 64% shrinking, related to a straight dipole. RFID chip fits inside a rectangle of 464.1x442 micrometers, barely visible to the naked eye. The tag is activated only by proximity to an active UHF-RFID reader from its RF field. The RF power block inside the tag converts the induced RF field to the DC voltage that triggers the biasing of the circuit for operation. For harvesting the RF energy, the auto-tuner maximized the power transfer from the antenna to the rectifier circuit. This adjustment occurs at power-up only and is held during operation. The input of the chip is symmetric with the $RF+$ pad connected to one antenna terminal and the $RF-$ pad

the other. The input is designed for symmetric devices like dipoles, but the main problem with the input configuration is the impossibility of being assisted by a DC bias from a battery for instance, or a PV cell. Assisted tags with DC bias are referred to as semi-passive tags and could cover a higher area than the passive normally could cover. In the case of the EM4325 chip, this assistance is available. The use of a battery could be an option but an external RF rectifier or a solar panel could be the most suitable solution for green energy IoT. The RF rectifier inside the M6 chip can't make the difference before DC-biasing between the RF coming from the reader or another RF source in the 860 to 960 Mhz range. Any RF source in this radio band can contribute to the DC biasing but the chip modulator/demodulator could be triggered only by the reader according to the handshaking protocol. This is not a problem if an additional DC output source helps to trigger the modulator/demodulator block as in the case of the EM4325 IC. In the case of DC-biased assisted mode, this chip offers extended reading range and reliability compared to the case in which the RF signal is the only one used for DC-biasing. A small PV cell could be used very efficiently like the ones made by Panasonic. This encapsulation confines inside a small rectangle of about 4x14 cm, which is suitable as a physical support for the RF antenna. The antenna will be even smaller and will allow a marginal surface around it to permit the illumination of the PV panel. The panel is also light and thin the thickness being up to 1 mm.

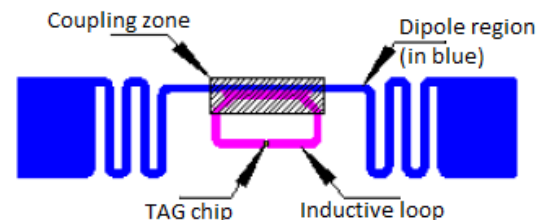


Figure 1. Sketch of an ordinary tag antenna.

In figure 1 a basic sketch of a tag antenna is depicted from scratch. Antenna, as one can see, consists of three main components. The tag chip is the most important one because the other two components are designed in accordance with its electrical properties. The inductive loop compensates for the capacitive inductance of the most tag chips available on the market. A conjugate match between the capacitive input impedance of the chip and the inductive impedance of the antenna has a key role in the power transfer. This is done inside the M6-P RFID tag by controlling a varactor diode. Mitigating the reflections, the chip can also efficiently harvest the RF power from the reader and convert it into the DC power for biasing the chip. More power efficiency means in general a larger detection range. The coupling zone is responsible for the RF energy transfer and with the reflection loss. The approach in figure 1 is looking for a medium coupling between the dipole and the tag chip. A smaller coupling will enlarge the bandwidth of the antenna. The optimization of the two parameters is made in HFSS during the simulation process. The most important component is the dipole. In figure 2 one can easily see that the dipole is protracted to confine a smaller rectangle. The smaller the antenna the better it fits the needs of the user. In this paper

the proposed antenna shown in figure 2 has asymmetric arms unlike the ordinary one from figure 1.

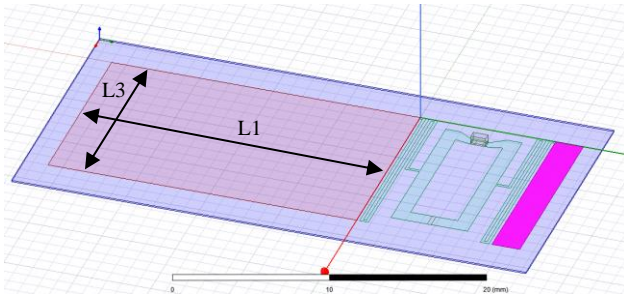


Figure 2. The tag UHF-RFID antenna in HFSS.

In this way the left patch of the dipole is larger and is designed to be transparent. An ordinary tag has both arms symmetrically placed and made of a thin sheet of silver. Transparency of the most important arm will allow the PV panel to generate more DC power. The PV panel also worked as a physical support for the antenna.

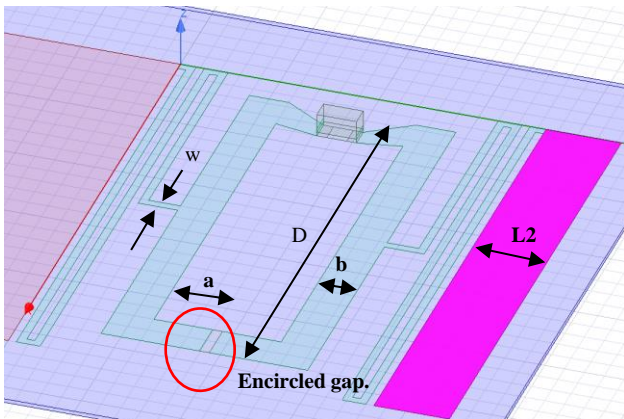


Figure 3. The loop and meander line antenna.

This experiment is available for a passive tag manufactured by Monza (R6-P). The tag and the antenna were manufactured for this chip but unfortunately it does not have the DC biasing module.

Table 1. UHF-RFID antenna dimensions in millimeters

L1	L2	L3	a	b	D	w
21	1.9	13	1.5	1	11.2	0.2

For the sake of the simplification the R6-P chip has been replaced with EM4325 IC on the antenna platform used by Monza. This new chip from Panasonic has almost the same dimensions of roughly 1.5x1 squared millimeters. The left side of the rectangular shape was cut out and replaced with a transparent sheet made of AgHT-tape. This sheet has a conductivity smaller than silver. The smaller conductivity will introduce some loss compared with pure silver. Nevertheless, this tradeoff will increase the power efficiency with the help of the PV-panel. Transparency will allow the visible light to go through the left arm of the dipole antenna and supply with the DC from the PV-panel. The right arm is smaller and has a negligible effect in

feeding blockage. The loop is transparent in the middle and insignificant due to its thin wire. Even though the new chip from Panasonic has a different parasitic capacitance slightly different from the Monza chip. To mitigate this problem a small gap was placed at the bottom of the loop. The gap was cut out from the Monza tag with a cutter. This encircled gap from figure 3 will increase the parasitic capacitance to fit the difference between the chips.

III. ANTENNA OPTIMIZATION

The simulation of the antenna is mandatory to optimize the use of the PV-panel. The PV is from polyester with relative electric permittivity equal to 3.4. This substrate will alter slightly the resonance of the antenna. The gap will be adjusted to compensate. The program can simulate the input impedance of the chip easily. The series resistance is 1200 ohms and its capacitance placed also in series is about 2.44 pF. To seek the parasitic capacitance, it was referred as C_p . This parameterization will allow the simulation of the impedance matching as the chip is working. When the tuner inside the chip finds the resonance, the conjugate matching will maximize the energy transfer from the RF to the chip.

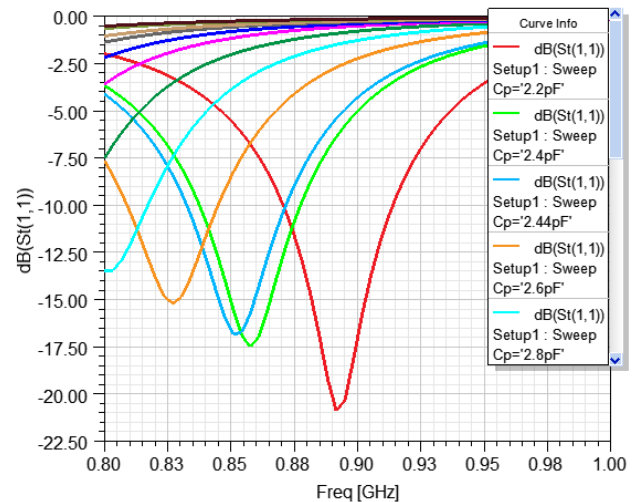


Figure 4. Reflection coefficient ($S_t(1,1)$) versus frequency using a logarithmic scale.

As can be seen in figure 4 the reflection coefficient at the input terminal number 1 varies with parasitic capacitance of the EM 4325. The tuner can adjust this capacitance with small steps of 0.2 pF with the help of some internal programmable registers. The capacitive gap has its role to compensate for the change made when the chip has been replaced. The smaller value of the reflection coefficient the better. In figure 4 the best results stand for the frequency which is near the middle of the band in-between 800-1000 MHz. Here the European band has been chosen between 800-900 MHz. Unlike Monza which cover both American and European band between 800 to 1000 MHz, this chip can cover only one. The problem comes from the parasitic capacitance of the gap which is too high. A smaller one has been beyond the available technology of the current experiment (a slit made with a cutter). A smaller gap under 0.2 mm could be possible in other circumstances, anyway for the sake of the experiment is acceptable. Without the gap the tuner will operate only between 900-1000 Mhz

only complying the American standard. The threshold considered as the limit for an acceptable value for the reflection coefficient lies on -10 dB. Normally if we multiply the parameter $S_t(1,1)$ from figure 4 with minus one we get the return loss. Every time the tuner matches the input impedance of the antenna the $S_t(1,1)$ trace from figure 4 drops to a minimum.

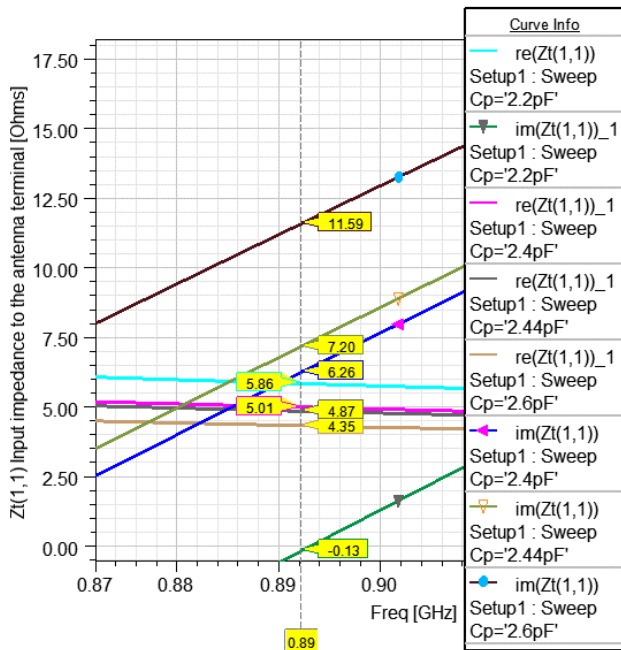


Figure 5. The real and imaginary part of the antenna input impedance versus frequency.

Every minimum from figure 4 marks a resonance in figure 5 outlined by the imaginary part of the input impedance. Unfortunately, when the electrical length of the dipole antenna is near the Chu-Harrington limit the real impedance is very small. This will increase the input current and loss. Here in the plot from figure 5 the real part of the input impedance is only around five ohms. Normally a dipole exhibits 73 ohms when its length tends to half wavelength. For 1Ghz this is 15 cm which is too much for a tag. Shrinking the antenna has an effect over the radiation pattern. The straight dipole emanating electromagnetic waves along the two lobes, as long as in this case the shape of the lobes is distorted as one can see in figure 6. Azimuthal radiation pattern when the phi angle is constant exhibits almost the same shape as the dipole does. In H plane when theta angle is constant zero the antenna exhibits an omnidirectional radiation pattern. This is not quite an advantage because the tag will be positioned vertically. This will exhibit rather a directivity in the horizontal plane where the reader initiates the interrogation of the tag. Maximum gain is around 2.2 dB, as the gain of the straight dipole. The tag does not suffer much after arms are retracted from this point of view. Radiation efficiency is good despite the minimization of the effective area of the tag. The active rectangle of the size L1xL3 from figure 2 undertake this job successfully. This enlargement of the radiation area is the point in the design of microstrip patch antennas which also have good gains. Nevertheless, this

asymmetry of the arms decreases the bandwidth as could be seen in figure 4.

Another issue that must be outlined here is the difficulty to measure at least the return loss with a Vector Network Analyzer to evaluate the differences between the reflection coefficients in figure 4 (like measurements versus simulations). If one uses a VNA connected to the antenna terminals instead of the UHF-RFID chip, then must use a trans-match to compensate the effect of the chip which in normal circumstances take part in the antenna system and affects resonance. Another difficulty when addresses this issue is related to the 50 Ohms resistive output impedance of the VNA against only 6 Ohms radiation impedance of the antenna. An inductive coupling could resolve the issue and can allow the chip to remain connected to the antenna terminals during measurements. Even though the parameter S11 does not follow the same behavior as the one from figure 4, due to the fact this shows the energy exchange between the antenna and the chip as long VNA will exhibit an S11 between the antenna and itself. We must agree the important role of the simulator here. To mitigate this problem, Monza integrates an auto tuner inside the chip that manages the energy exchange during the hand shaking process. This is possible when the measuring device is placed inside the load and is an integrated part of the system.

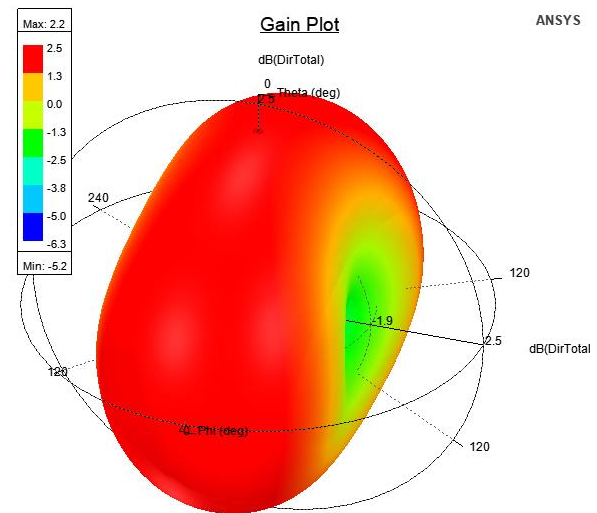


Figure 6. 3D radiation pattern (total gain in dB) of the antenna.

IV. MEASUREMENTS AND PROTOTYPING

In figure 7 is shown the prototype comprises one Raspberry Pi version 3 and one Arduino uno as mainboard for the RFID shield. The shield board for the Arduino uno is made by Sparkfun based on the M6E-Nano RFID chip. This board is Arduino-uno compatible and can be programed using Arduino language. This is an affordable solution to have a benchmark to evaluate some RFID tags or RFID antennas. From the Arduino-uno, data is transferred via serial port to the Raspberry Pi. The data management is made with the help of python easily. Some parameters that are related to the transmitted power or standardizations are also made from python. The power is adjustable from 0 to 27 dBm (from 1mW to roughly 1W) which means that with

the use of the original Sparkfun antenna (from figure 8) a tag could be read up to 5 meters. The external antenna overrun the existing one, integrated on the board. The directivity of the external antenna is 14dBi an increase of about 10 dB in comparison with the onboard antenna. This will increase the effective radiated power ten times. With the onboard antenna which is an inverted-F, the detection range is 10 to 20 cm. With the external antenna the range is extended from 0.2 meters up to 5 meters, twenty times. Inside the box (figure 8) is an array of four elements (2x2 uniformly distributed rectangular array - URA). Each element is represented by a bi-quad type, made in microstrip technology.

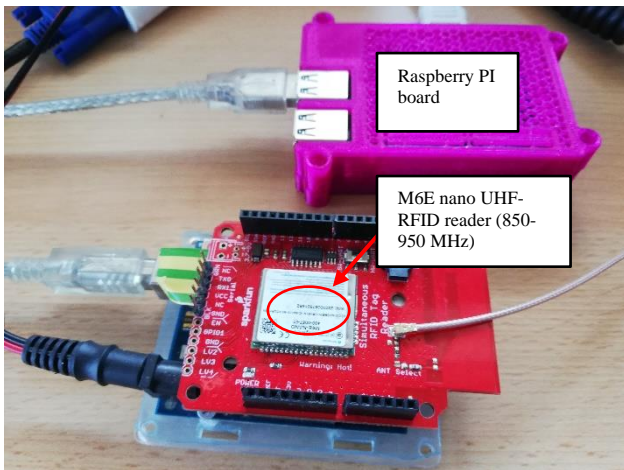


Figure 7. The benchmark used to evaluate tag performance.

In figure 10 one can see the tag which was used for the experiment and simulated in HFSS. The UHF-RFID antenna is printed on paper using a thin layer of silver. The size of the tag is around 5x2 cm, taking in account the paper stick margin.

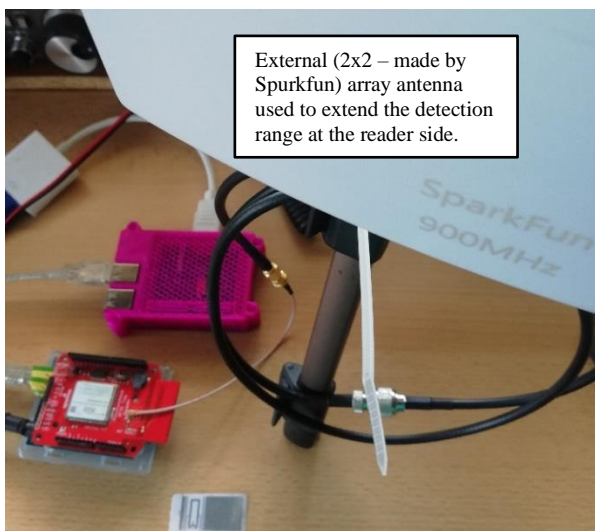


Figure 8. External array antenna for detection range extension (made by SparkFun).
The original Monza R6-P RFID chip has been replaced

with EM4325 IC. As one can see in figure 9 and 10 the upper side of the antenna arm has been cut out. Instead of the upper arm a transparent conductive tape, made by HT silver has been used. Using the sticky side of the tag the tape is pressed over the remaining silver arm upon the solar cell from figure 11 as a rigid support. The antenna layer is upside down and invisible to the user. The new label having the antenna under the paper can be used to print information related to the product on which the tag will be attached. The small slit, marked in figure 10 with a bolded circle, compensates for the parasitic capacitance of the new chip and avoids the shorting of the PV panel by blocking the DC. The DC voltage when the solar cell will be exposed to the visible light is 1.5V. This will be enough to trigger the chip and extend its detection range. The range is extended after measurements from 5 meters up to 12 meters even if the light is coming from artificial sources.

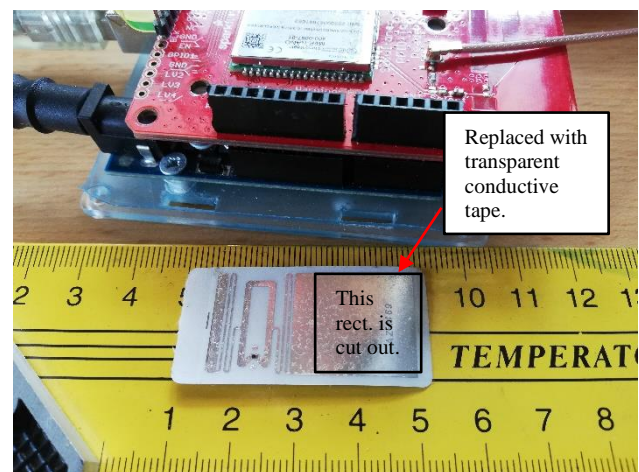


Figure 9. Printed tag.

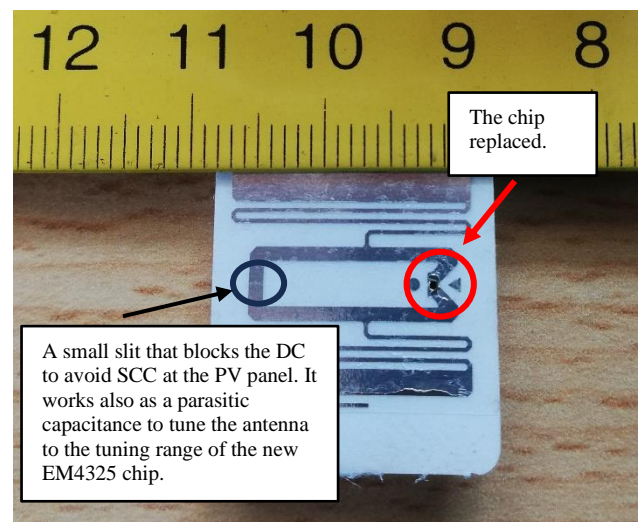


Figure 10. Adjustments made to compensate the parasitic capacitance of the EM4325 IC chip.

Unfortunately, over 12 meters the detection range drops suddenly no matter how much the solar cell is exposed. This is probably normal due to the reader's sensitivity. Figure 11 shows the way in which the antenna at the tag

side accommodates to the dimension of the PV panel. The sticker is pressed against the panel and in between a multi lines flexible ribbon cable has been used. This is a good choice because between two plastic layers there are 50 to 60 Ohms characteristic impedance lines in coplanar configuration apart from one another at about 0.2 mm. The ending side has exposed silver coated pins that allow the connection with the antenna terminal. To mitigate the coupling with the antenna, the length of the ribbon cable is one quarter of the wavelength, calculated at 900 MHz (roughly 8.3 cm). According to the microwave transmission lines theory every time when at one end of a quarter wavelength line is an impedance that stands close to zero, at the other end one can get much higher impedance. In this case the ribbon cable works as an impedance transformer. At the antenna side is roughly 5 to 6 Ohms and at the PV panel the impedance is much higher of about 500 Ohms. This transformation stands only for RF wave that is seeing a higher impedance toward the PV panel than the impedance seen toward the chip. Normally the RF will choose to follow the path toward the chip. In DC the line behaves like a short circuit that allows the DC biasing of the chip by the PV output terminals with 1.5 V.

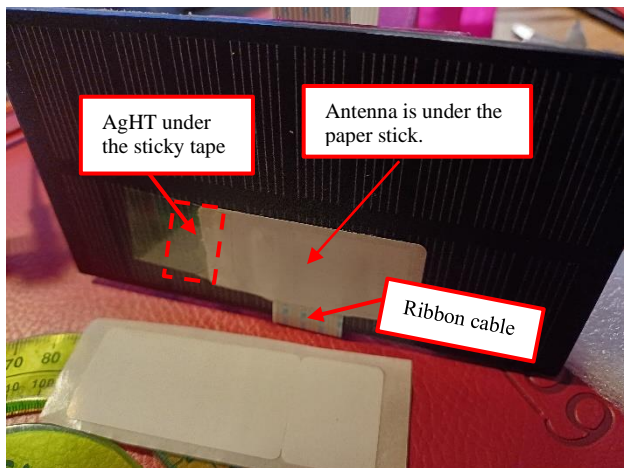


Figure 11. PV-panel from Panasonic (6x12 cm – 1.5 V DC)

The paper stick maintains the pressure with the ribbon cable and an additional sticky transparent tape has been used to press the transparent tape in the rectangular marked in figure 11 with a dash line. Unfortunately, the ribbon cable is not flexible enough to keep the pressure, so an additional plastic clamp is used (is not shown here).

V. CONCLUSIONS

In this paper a new approach is proposed to use a semi-active UHF-RFID tag based on a solar cell to extend the detection range of the reader. Here a benchmark based on SparkFun UHF-RFID reader has been designed. The evaluation of the tag performance is made using a Raspberry Pi board programed in python to manage data transferred from the Arduino-uno board. The tag was modified to accommodate the constraints of the new chip that supports the DC bias, for detection range extension. These modifications are detailed in the paper and are assisting the reader to identify the tag from at most 12 meters. Without this modification the tag identification is under 5 meters if an external antenna is used. For further development of the tag identification assistance, it is intended to attach an electrolytic capacitor because the PV cells are in fact photo diodes that allows the current flow in only one direction. This will delay the electrical discharge of the electrolytic capacitor and will preserve the energy during night when PV is off grid. For the moment even if this improvement can prolong the operational time of operation at the tag side, is not feasible if the electrolytic capacitor is not planar and does not conform to the shape of the PV panel. A low voltage conformal electrolytic capacitor would allow higher capacitance and low loss. This would pave the way toward green IoT.

REFERENCES

- [1] D. M. Dobkin, *The RF in RFID Passive UHF RFID in Practice*, Library of Congress Cataloging-in-Publication Data, 2007, U.S.A., pp 361-440.
- [2] T. F. Thompson, *Detecting means for stolen goods*, US Patent US2774060 A, 1956.
- [3] P. H. Cole, R. Vaughan, *Electronic surveillance system*, US patent US3706094, 1972.
- [4] I. Jalay, I.D. Robertson, "RF barcodes using multiple frequency bands", *Microwave symposium digest*, 2005, LE MTT-S Internat., pp 4.
- [5] J. McValay, A. Hoorfar, N. Engheta, "Space-filling curve RFID tags" *Radio and wireless symposium*, 2006 IEEE, pp 199-202.
- [6] M. Manteghi, S. Rahmat, "Frequency notched UWB elliptical dipole tag with multi-bit data scattering properties" *Antennas and Propagation Society International Symposium*, IEEE, San Diego, pp. 789 - 792, 2007.
- [7] Wenxing An, Hui Wang, Yu Lou, "Dual-Band Antenna Integrated with Solar Cells for WLAN Applications", *Front. Phys.*, 08 October 2021, Sec. Optics and Photonics.
- [8] Arpan Desai, Trushit Upadhyaya, Jay Patel, Riki Patel, Merih Palandoken, "Flexible CPW fed transparent antenna for WLAN and sub-6 GHz 5G applications", *Microwave and Optical Technology Letters*, 03 february 2020, <https://doi.org/10.1002/mop.32287>.
- [9] George Altemosel, "Achieving Cell Balancing for Lithium-Ion Batteries", *Hearst Electronics Products*, 2008. [Online]. Available: <http://www2.electronicproducts.com/> [Accessed: May 1, 2010].